Int. J. Heat Mass Transfer. Vol. 34, No. 3, pp. 739–748, 1991
Printed in Great Britain

0017-9310/91 $3.00 + 0.00
Pergamon Press plc

Turbulent flow measurements in a 30/60 degree right triangular duct

K. S. HURST†‡ and C. W. RAPLEY†

†School of Mechanical and Manufacturing Engineering, Sunderland Polytechnic, U.K.
‡Department of Engineering Design and Manufacture, University of Hull, North Humberside HU6 7RX, U.K.

(*Received* 7 *June* 1989)

Abstract—Experimental data are reported for fully developed turbulent flow in a right triangular duct with internal angles of 60 and 30 deg. This duct geometry has no symmetry planes and as such generates a type of non-circular duct flow for which data are scarce. Measurements are made with hot-wire anemometry in an air flow rig specifically constructed for the tests. The friction factor characteristic and axial velocity contours and profiles are presented, together with contours and/or profiles of turbulence intensity, turbulence kinetic energy and the Reynolds shear stresses. Where appropriate, comparisons of the profiles are made with data from measurements in other duct geometries. The presence and influence of turbulence driven cross-plane secondary flow is clearly evident and the implied circulations follow the pattern expected from previous measurements in other ducts.

INTRODUCTION

THERE is an urgent need for good quality turbulent non-circular duct data to assist with duct designs and with the development of numerical calculation procedures. The present work is aimed at helping to fill this need, with a study of turbulent flow through a 30/60 deg right triangular duct which has been chosen to fill an important gap in the available experimental data. The overwhelming majority of experimental non-circular duct studies have dealt with ducts that contain one or more symmetry planes. This has reduced the effect of the duct walls on the predictions so that in most cases a simplified one-dimensional approach could be taken in the wall region to yield acceptable results. With the present duct cross-section there are no symmetry planes so that the flow generated can be expected to be fully influenced by the duct walls and should provide useful data to test the traditional methods of dealing with the wall region and perhaps aid the development of new methods. No previously published experimental data for this duct shape have been found in the literature.

Hot-wire anemometry has been used for turbulent duct flow measurements now for many decades and is thus well established with standard equipment and methodology. Accepted data for fully developed non-circular duct flow have been published for square and rectangular ducts, triangular ducts, annuli, elliptical ducts and various rod bundle passages—see for example, ref. [1] for a summary of work published from 1950 to 1980.

From this and other data, the mean flow and turbulence characteristics of fully developed non-circular passage flows have been established. The mean flow characteristics are much influenced by the cross-plane secondary flow which is generated by the interacting turbulent stress fields that are present in non-circular passages. These secondary motions take the form of flows in the cross-plane from regions of high axial velocity (core) into regions of lower axial velocity (corners), recirculating back to the core via the wall regions so as to preserve cross-plane continuity. Typical circulations as predicted, and later confirmed by measurements, for an equilateral triangular duct [2] are shown diagrammatically in Fig. 1.

The convective effect of these circulations on axial velocity is to reduce core levels and increase corner region levels, i.e. to make the core velocity profile flatter than may be expected from circular duct measurements. This also gives rise to distortions in axial velocity contours which bulge into corner regions and are displaced from the wall in wall regions away from the corner. These distortions provided evidence as early as 1926 of the existence of secondary flows in non-circular ducts [3] and were found to be even more exaggerated in measured turbulence intensity and turbulence kinetic energy contours obtained from much later hot-wire and laser-Doppler investigations [2, 4, 5]. The Reynolds stress profiles, usually taken along mid-wall bisecting planes appeared to be less influenced by secondary flow when compared with circular duct measurements. The characteristic anisotropy of the cross-plane normal stresses in the wall-influenced region are generally similar to those in circular pipes, although the core and near wall levels may differ.

The friction factor characteristics are usually presented using the equivalent (hydraulic) diameter of the duct which appears to correlate most of the geometrically less extreme non-circular passages with circular duct data. Significant deviations from this

NOMENCLATURE

f	friction factor
k	turbulence kinetic energy [$m^2 s^{-2}$]
L_x, L_y	coordinates of maximum axial velocity [mm]
Re	Reynolds number
u, v, w	velocity components in the z-, x- and y-directions, respectively [$m s^{-1}$]
u', v', w'	fluctuating velocities [$m s^{-1}$]
$\overline{u'^2}$, $\overline{v'^2}$, $\overline{w'^2}$	kinematic Reynolds normal stresses [$m^2 s^{-2}$]
$\overline{u'v'}$, $\overline{u'w'}$	kinematic Reynolds shear stresses [$m^2 s^{-2}$]
u^*	mean friction velocity [$m s^{-1}$]
u_b	bulk velocity [$m s^{-1}$]
x, y	coordinates of cross-section [mm].

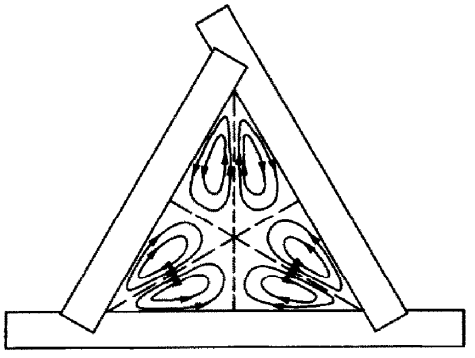

FIG. 1. Measured secondary flow circulations in an equilateral triangular duct [2].

appear to occur however with passages that have acute internal angles, such as isosceles triangular ducts with small apex angles and passages with cusped internal angles—as will be shown later.

The most recent and comprehensive experimental investigation of turbulent flow in triangular ducts appears to be that of Aly *et al.* [2], where detailed measurements of axial pressure drop, axial velocity, cross-plane secondary velocities, local wall shear stress and five of the six Reynolds stresses were made in an equilateral triangular duct, using a hot-wire anemometer. Measurements were taken in a one-sixth symmetry section of the duct which took the form of a 30/60 deg right triangular section with symmetry planes on two sides and the wall on the side between the 90 and 30 deg section angles—see Fig. 1. The measurements confirmed the expected circulation pattern of secondary flow, as shown diagrammatically in Fig. 1, which is from the core into the corners, returning to the core via the wall region. The maximum secondary velocities, of about 1.5% of the mean axial velocity, were found in this latter region. As may be expected, in the absence of any previously published data for the present 30/60 deg right triangular duct, the results from this equilateral triangular duct investigation of Aly *et al.* form one of the few possible comparisons with the present work so that more details and discussion will appear later.

THE TEST RIG

A schematic diagram of the test rig is given in Fig. 2, which shows the basis to be an open circuit 'blower' tunnel with air forced through the settling length, the long straight lead duct and main test section by an air blower located at duct entry. This allowed easy access to the main measurement section which was located inside the duct, 25 mm from the exit plane of the test section. The main disadvantages of this type of experimental set-up, those of probe contamination and of flow pulsations, etc. induced by the blower, were minimized by the use of a 5 μm inlet filter together with frequent routine re-calibrations of the probe (*in situ*), and careful design of the pre-test section which contained a flexible, blower isolating, pipe section, a flow measuring orifice and a settling chamber.

The sudden enlargement was used at the entrance

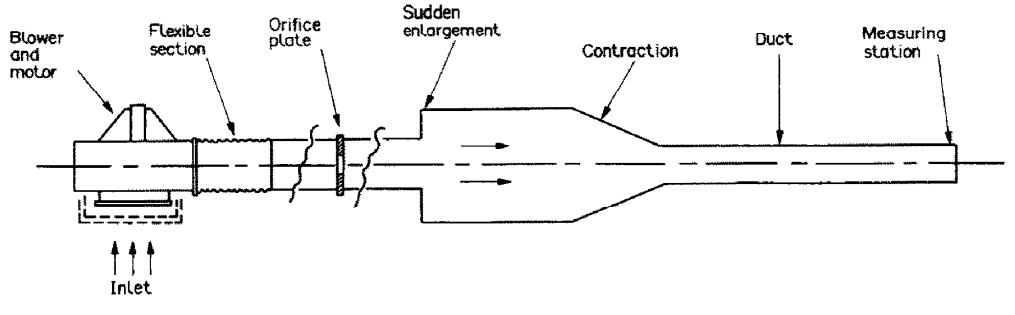

FIG. 2. Schematic view of test rig.

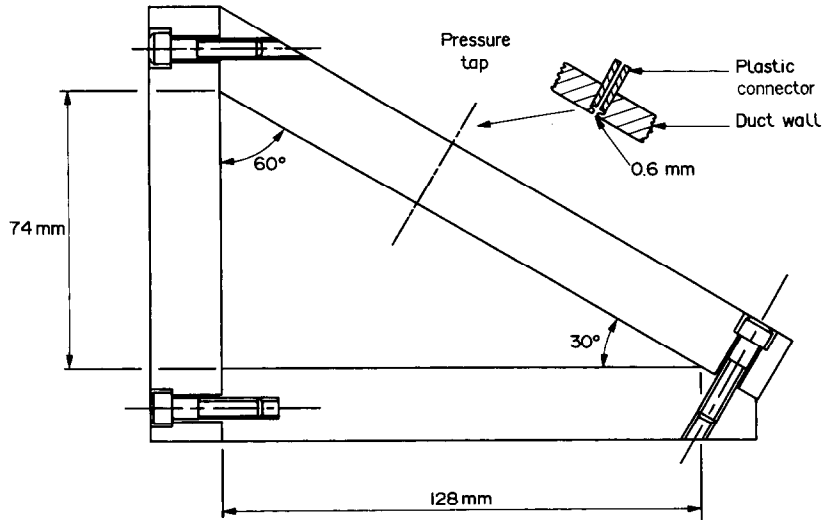

FIG. 3. Cross-section of duct.

to the settling chamber since the aim of smoothing the flow to near stagnation conditions could be achieved more compactly and efficiently than with the alternative of a wide angle diffuser. With the latter, the overall pressure losses are greater than a sudden enlargement when the included angle exceeds 40 deg. The contraction from this settling chamber to the test section also incorporates the transition from a circular to a triangular cross-section. The approach angle to the test section is 4 deg maximum with provision made for honeycomb flow straighteners at the entrance to the test section, which in the event proved unnecessary.

The main 30/60 deg triangular test section consists of an initial 3 m length lead duct made from 20 mm thick plywood followed by a final 1.5 m measurement length constructed from 20 mm thick precision acrylic ('perspex'), in three 0.5 m lengths and to the design shown in Fig. 3 with an internal tolerance of ± 0.2 mm. Straightness of the duct axis over the three separate lengths was measured to within a tolerance of 0.1 mm. A total length of 67 equivalent diameters was provided with this arrangement. This was considered long enough to ensure fully developed mean flow conditions at the exit according to previously published data which indicated that fully developed mean flow was achieved with lengths of 40 equivalent diameters for a square duct [6] and 61 diameters for an isosceles triangular duct [7] with an apex angle of 25 deg. Aly *et al.* [2] used an equilateral triangular duct test section

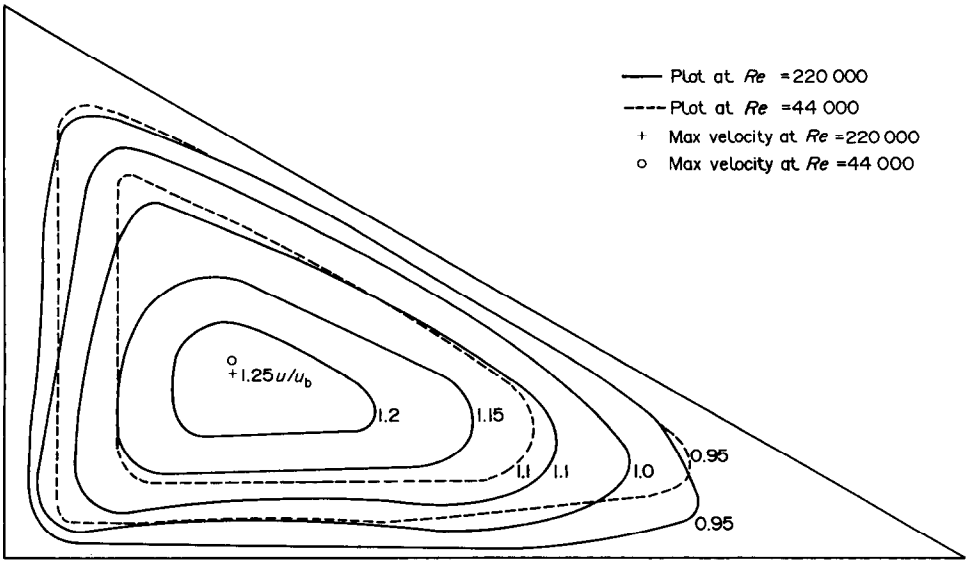

FIG. 4. Primary velocity contours at the measuring station.

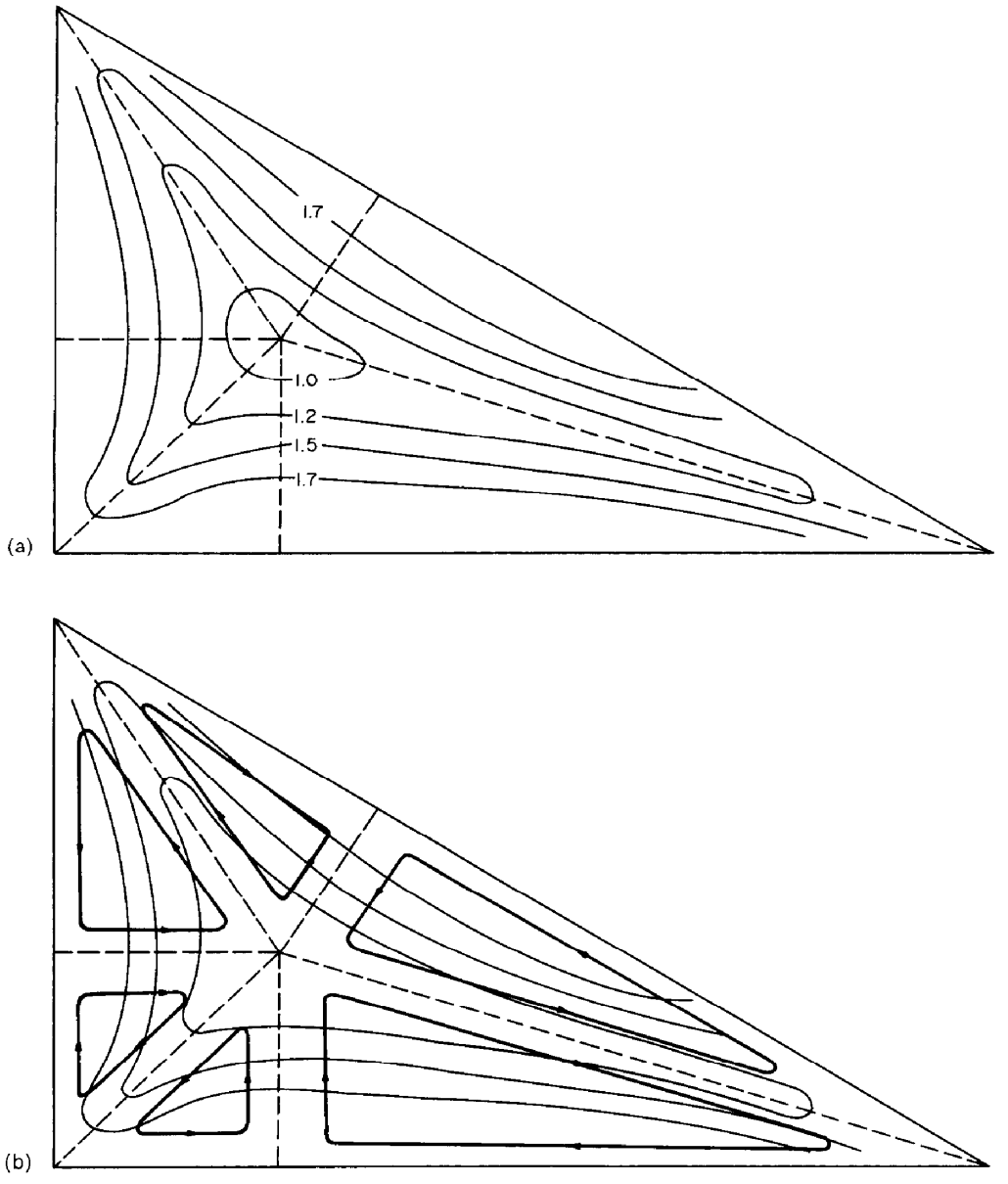

FIG. 5. (a) Contour plot of axial turbulence intensity $[\sqrt{(u'^2)}/u^*]$, $Re = 220\,000$. (b) Implied turbulence driven secondary flow circulations.

length of 133 equivalent diameters but did not report any information on the minimum length needed for fully developed mean velocity flow. However, this latter duct length is likely to have been enough to obtain fully developed normal stress fields in addition to fully developed mean flow.

Provision for the measurement of axial pressure gradient was made by locating static pressure tappings at 100 mm intervals along the final 23 equivalent diameters of the duct. These 15 pressure tappings were placed in the hypotenuse of the triangular duct, at a position to coincide with maximum near wall velocities. Also, at the measuring station, pressure tappings were placed in all three side walls, again at positions to coincide with maximum velocities. The final 0.5 m length of the acrylic section was made easily removable and the whole duct was designed such that it could be rotated through 90 deg, relative to the settling chamber, to enable some tests for fully developed flow to be made, as will be described later.

All local measurements were made with a hot-wire anemometer (DISA 55M series) working in the constant temperature mode and with a linearizer. Axial mean and fluctuating velocities were measured with a standard single wire probe, normal to the flow, whereas the cross-plane fluctuating velocity components were measured with a single slant wire (45 deg to the flow) probe. The latter was also used to check axial component measurements. The probes were clamped in a standard DISA traversing mech-

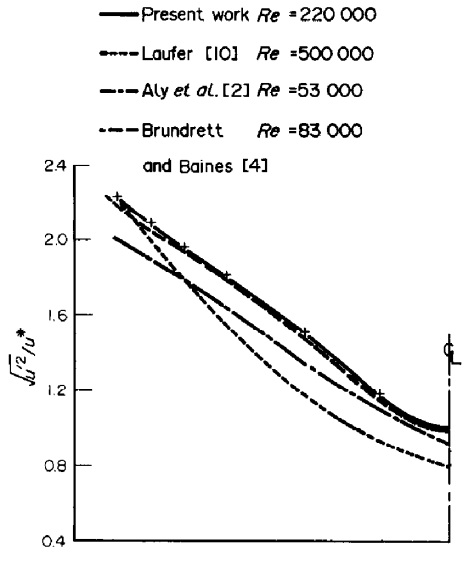

FIG. 6. Axial turbulence intensities along mid-wall bisector.

anism, which in turn was mounted on a standard mechanical travelling microscope, equipped with vernier scales that enabled positioning in the duct cross-section to within ± 0.01 mm. Provision was also made for a 1 mm internal diameter pitot tube to be substituted for the hot-wire probe for calibration purposes. Pitot tube pressure measurements were made with a projection micromanometer which had a resolution of 0.02 mm water.

The repeatability of all of the readings taken was found to be complete and the overall accuracy of the primary velocity measurements was estimated at $\pm 2.4\%$. Near wall corrections were found not to be necessary since the nearest approach of the probe was 2 mm when the limiting furthest distance from the wall that would require correction was estimated at 0.25 mm [8]. The overall accuracy of the stress measurements was estimated at $\pm 6\%$ for axial components and $\pm 16\%$ for cross-plane components. The overall accuracy of the volumetric flow rate returned by the orifice plate meter was estimated at $\pm 2.7\%$ for the lowest Reynolds number of 44 000, and $\pm 2\%$ at the highest Reynolds number of 220 000. More details of the test set-up and the accuracy estimates can be found in ref. [9].

EXPERIMENTAL RESULTS

Initial tests were made to check how fully developed the flow was at the measurement plane. A linear axial pressure gradient was obtained along the acrylic section, indicating that there was no marked entrance effect. Two other separate tests were made using measured local axial velocity distributions, one at 10 hydraulic diameters upstream (by removing the final 0.5 m section) and the other at the usual measuring station, but with the whole duct turned through 90 deg relative to the inlet settling chamber. In both cases local velocities were within the experimental error of the measurements at the measuring station, indicating that, within the capabilities of the measuring system, fully developed mean flow had been achieved.

Tests were made over a range of Reynolds numbers and detailed tables of the results obtained are given in ref. [9]. From these tables, contour plots have been interpolated and used here to display more clearly the main characteristics of the flow.

Measured axial velocity contours at the two extreme Reynolds numbers are shown in Fig. 4. These are normalized with the mean axial velocity and show, as may be expected, greater penetration of the flow into the decreasingly acute corners, as well as a sig-

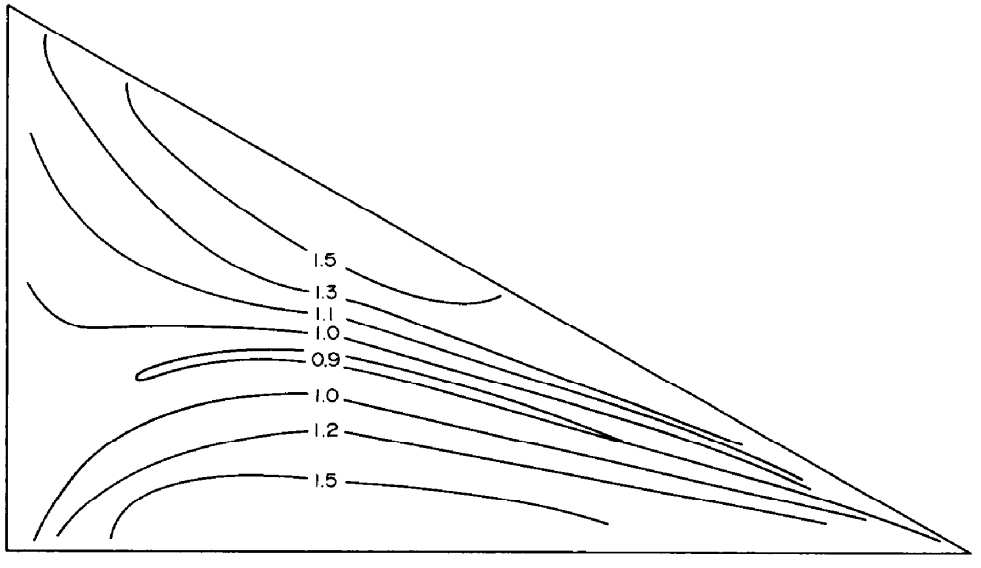

FIG. 7. Contour plot of turbulence intensity $[\sqrt{(v'^2)}/u^*]$, $Re = 220\,000$.

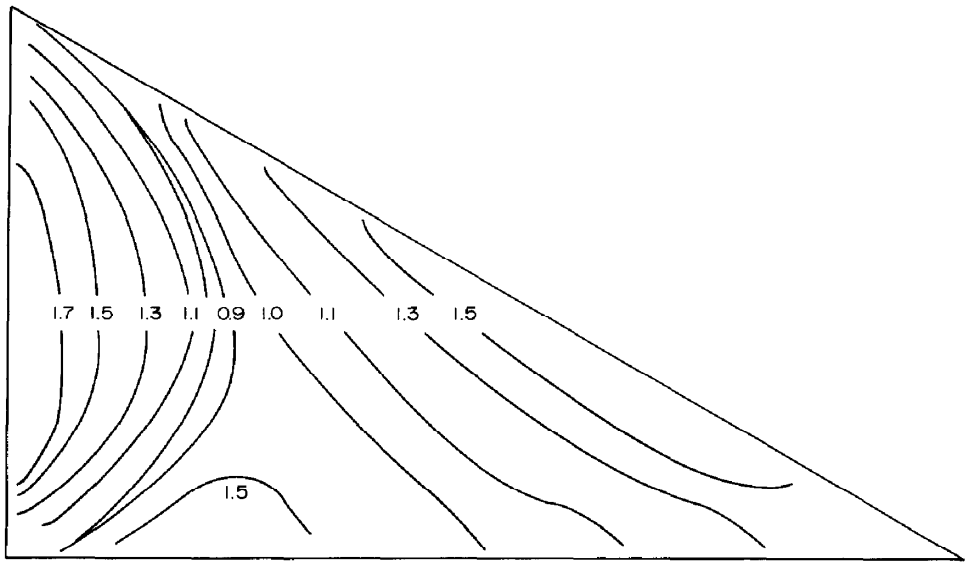

FIG. 8. Contour plot of turbulence intensity [$\sqrt{(w'^2)}/u^*$], $Re = 220\,000$.

nificant Reynolds number dependence away from the core. However, in the central core region, representing some 80% of the flow area, the normalized velocity distributions at the other Reynolds numbers showed similar trends to those plotted. Some evidence of secondary flow influence can also be seen with the contours bulging into the corners and drifting away from the wall around the mid-wall region.

The above secondary flow effects are much more obvious in the axial turbulence intensity contours shown in Fig. 5(a). Little difference was found between the normalized intensity contours for different Reynolds numbers so that results for only one Reynolds number are shown. The implied turbulence driven secondary flow circulations are clearly those shown schematically superimposed in Fig. 5(b). The convective transport effect of these cross-plane flows on local axial velocity moves the contours in the direction of flow, as indicated by the contours pushing into the corners and moving away from the walls in the wall region, are most clearly marked. An attempt was made to derive the cross-plane secondary velocities from the hot-wire measurements, but the results obtained were too scattered to show any trends that could add anything further to the above deductions.

Axial turbulence intensity profiles between the wall and the core along the mid-wall bisectors, bounding the 90 deg corner, are compared with measurements in other ducts in Fig. 6. The shape and slope of the profile measured by Laufer [10] in a circular duct is different from those for non-circular ducts, including the present one, which lies above the equilateral triangular duct profile of Aly *et al.* [2] and agrees with the square duct profile of Brundrett and Baines [4], which has the nearest Reynolds number to the present work, and has similar core levels.

Contour plots of the transverse turbulence intensities are shown in Figs. 7 and 8 with mid-wall bisecting plane profiles compared with profiles from other ducts in Fig. 9. The expected similarities in contour shape of each component relative to the different walls at right angles are clearly evident (each component is of course, normal [e.g. $\sqrt{(v'^2)}$] to the wall in one plot whilst being parallel [e.g. $\sqrt{(w'^2)}$] to the same wall in the other). Although the core levels of transverse intensity are similar to those measured by Aly *et al.*, the wall region levels are much higher in the present work, as seen in Fig. 9. In addition, the damping effect of the wall on the transverse stress is more significant in the Aly *et al.* equilateral triangular duct measurements and also the Brundrett and Baines measure-

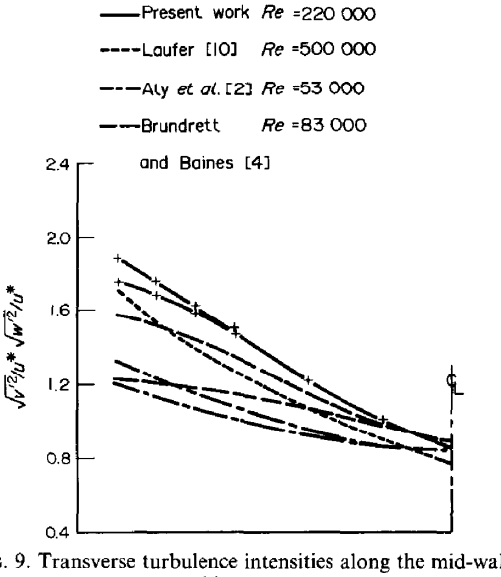

FIG. 9. Transverse turbulence intensities along the mid-wall bisector.

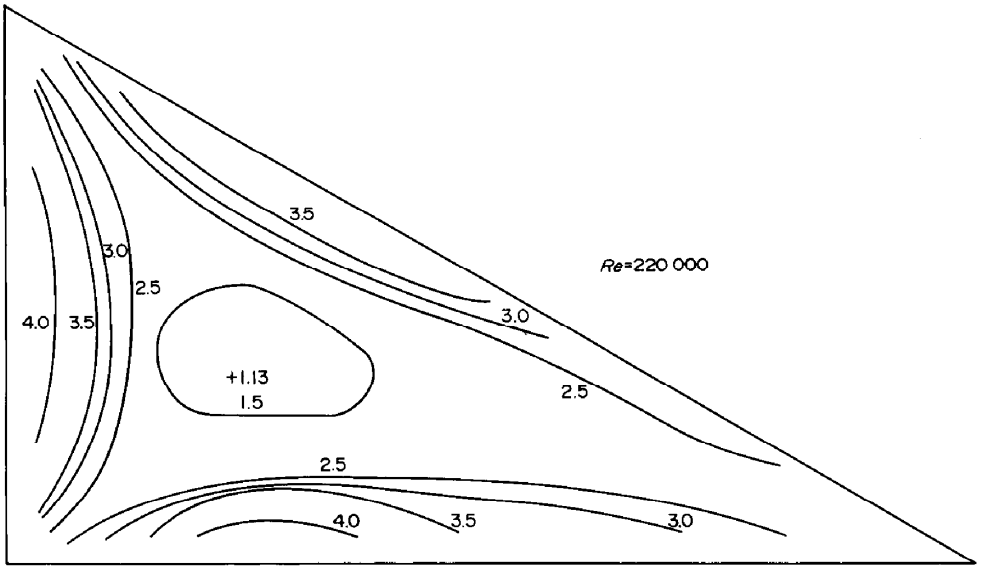

FIG. 10. Turbulence kinetic energy contours normalized by friction velocity, $Re = 220\,000$.

ments in a square duct. The differences between profiles here are perhaps as much due to uncertainties in the measurements as to differences in duct shape.

The combined intensities are presented in the form of turbulence kinetic energy contours and profiles in Figs. 10 and 11. These show the expected effects due to the marked differences in turbulence energy generation in the core, with its low velocity gradients and generation rates, and the wall regions with their high velocity gradients and generation rates. The contours also show the convective transport influence of the cross-plane secondary flows in pushing the core levels towards the corners through the region around the corner bisectors. The profiles in Fig. 11 indicate that

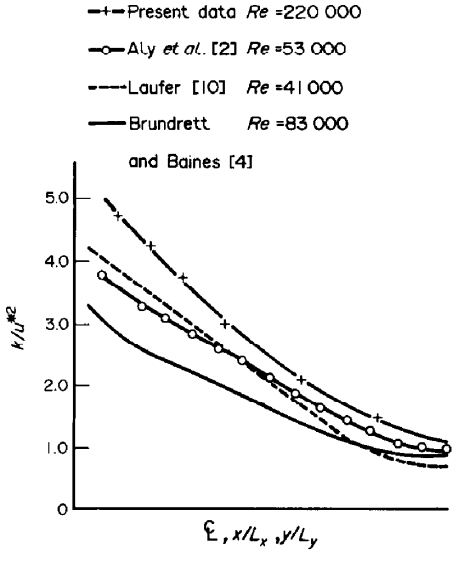

FIG. 11. Turbulence kinetic energy (k/u^{*2}) along mid-wall bisector.

the present work has recorded much higher near wall turbulence kinetic energy levels than those found in the equilateral triangular duct of Aly *et al.* and the square duct of Brundrett and Baines. Careful checks on instrumentation and data evaluation did not reveal any systematic error in the present work so the conclusion is that the higher levels of turbulence energy are more likely due to shape effects than to the higher Reynolds number of the duct although normalizing with friction velocity does not necessarily give the Reynolds number dependence often assumed.

Contours of the two measured Reynolds (axial) shear stresses are plotted in Figs. 12 and 13. Once again, as expected, the 90 deg similarity of contours is evident, giving contour patterns as may be expected from previous measurements [2, 4]. The small regions of negative stress in regions near to mid-wall where positive or zero stress may be expected, have also been detected in other shaped ducts, such as the square duct of Brundrett and Baines [4] and the equilateral triangular duct of Aly *et al.* [2]. Repeated measurements in these negative regions with a variety of probes confirmed their existence in the present work. It is suggested by Aly *et al.* that these negative regions are connected with the convective effects of secondary flow away from the wall which influence the local axial velocity gradients in this region. Although no secondary velocities were measured in this work, this is consistent with the implied circulation shown in Fig. 5(b).

Finally, the measured friction factors are shown in Fig. 14 where they are compared with measurements from a variety of other shaped passages. The present values are consistent with those of Aly *et al.* for the equilateral triangular duct, being about 10% lower than the values given by the Blasius relation for smooth circular pipes ($f = 0.079/Re^{1/4}$). The in-

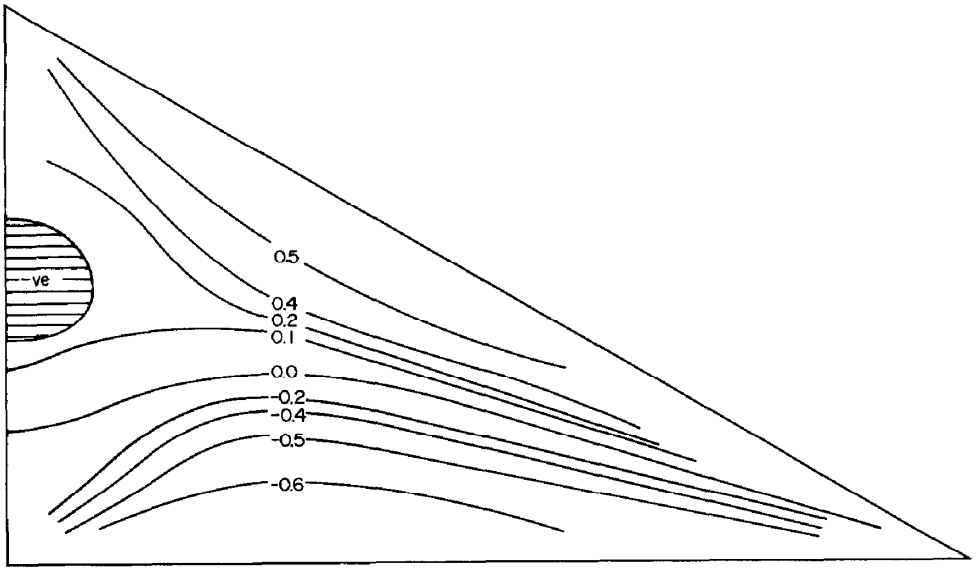

FIG. 12. Reynolds shear stress contours ($\overline{u'v'}/u^{*2}$), $Re = 220\,000$.

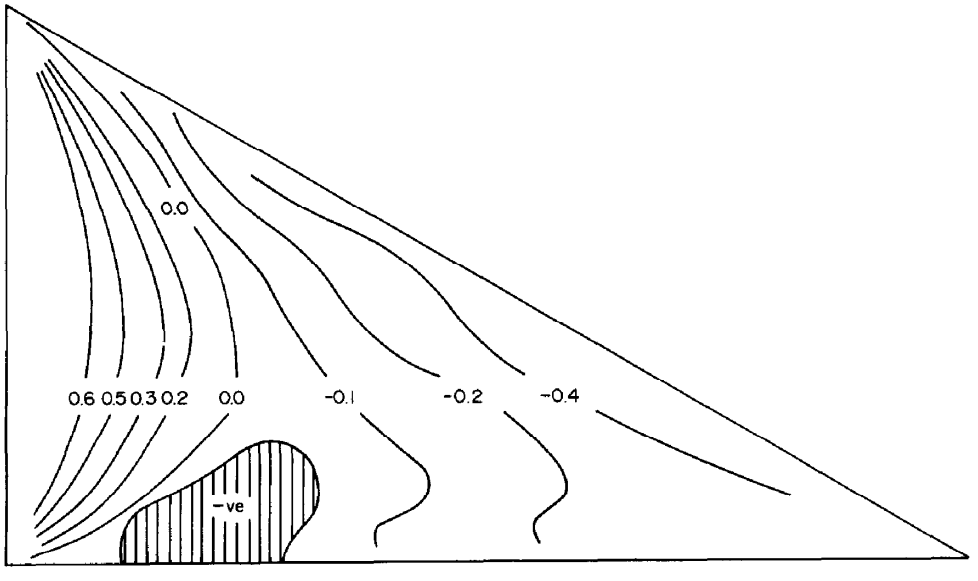

FIG. 13. Reynolds shear stress contours ($\overline{u'w'}/u^{*2}$), $Re = 220\,000$.

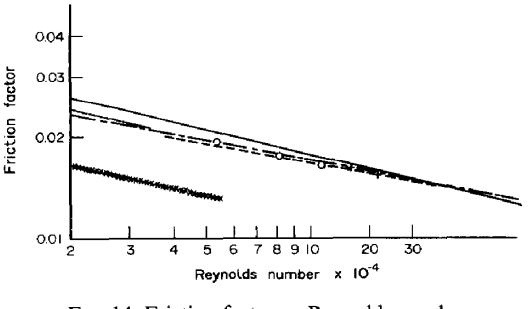

FIG. 14. Friction factor vs Reynolds number.

adequacy of the equivalent (hydraulic) diameter in correlating non-circular duct friction is clearly evident here with, as may be expected and previously mentioned, the acute internal angled and cusped ducts deviating the furthest from the circular duct values. The Malak *et al.* [11] 'universal' non-circular duct correlation tends to under-predict this case.

CONCLUSIONS

Measurements have been presented for axial mean and fluctuating velocities and cross-plane fluctuating

velocities in fully developed turbulent flow in a 30/60 deg right triangular duct. To the authors' knowledge, these are the first such measurements presented for this duct shape and indeed for a triangular duct without symmetry planes. The results were mainly given in the form of contour plots for easier visual appreciation of the turbulent flow characteristics with some profile plots for comparison with measurements in other duct geometries. The contour plots clearly revealed the influence of the turbulence driven secondary flow on the local characteristics.

The bulging of axial mean velocity and turbulence intensity contours into the duct corners and the drifting away of contours from the duct walls in regions away from the corners enabled a clear picture of the implied secondary flow circulations. These were from the core into the corners along the corner bisecting plane region, recirculating to the core via the wall region and planes normal to the wall near mid wall, in a series of counter-flowing circulations around the duct. This is entirely consistent with the secondary flow circulations found in other shaped ducts, being in a direction from the region of highest axial velocity into the regions of lowest axial velocity, recirculating back to the core in counter-flowing circulations to preserve continuity.

Comparisons of turbulence profiles with measurements in other duct geometries revealed that the levels found in the present work were generally higher than those in previous ducts, particularly in the wall region. The main difference, other than geometry, was the significantly higher Reynolds number in the present work. It appears that normalizing with friction velocity, as conventionally used, does not provide the independence from Reynolds number often assumed.

The measured friction factors were consistent with those at lower Reynolds numbers for the equilateral triangular duct and about 10% below the circular duct levels.

The results presented fill an important gap in turbulent duct flow data, in that the duct does not have any symmetry planes and provides a flow field that is a combination of those found in the symmetrical square and equilateral and isosceles triangular ducts. This should be of interest to designers involved with flow in non-circular passages and to developers of prediction methods for this class of flow.

REFERENCES

1. C. W. Rapley, A summary of experimental turbulent non-circular passage flow and heat transfer, Report FS/80/41, Dept. Mech. Engng, Imperial College, London (1980).
2. A. M. Aly, A. C. Trupp and A. D. Gerrard, Measurement and prediction of fully developed turbulent flow in an equilateral triangular duct, *J. Fluid Mech.* **85,** 57 (1978).
3. J. Nikuradse, Investigations on the distribution of velocity in turbulent flow, *VDI ForschHft.* 281 (1926).
4. E. Brundrett and W. D. Baines, The production and diffusion of vorticity in duct flow, *J. Fluid Mech.* **19,** 375 (1964).
5. P. Carajilescov and N. E. Todreas, Experimental and analytical study of axial turbulent flows in an interior subchannel of a bare rod bundle, *Trans. ASME, J. Heat Transfer* **101,** 628 (1976).
6. L. C. Hoagland, Fully developed turbulent flow in straight rectangular ducts, Ph.D. Thesis, M.I.T. (1960).
7. E. R. G. Eckert and T. F. Irvine, Flow in corners of passages with non-circular cross-sections, *Trans. Am. Soc. Mech. Engrs* **78,** 709 (1956).
8. J. C. Bhatia, F. Durst and J. Jovanovic, Corrections of hot wire anemometer measurements near walls, *J. Fluid Mech.* **122,** 411 (1982).
9. K. S. Hurst, Measurement of turbulent flow characteristics in a 60/30 degree triangular duct, M.Phil. Thesis, Sunderland Polytechnic (1987).
10. J. Laufer, The structure of turbulence in fully developed pipe flow, NACA Report 1174 (1951).
11. J. Malak, J. Hejna and J. Schmid, Pressure losses and heat transfer in non-circular channels with hydraulically smooth walls, *Int. J. Heat Mass Transfer* **18,** 139 (1975).
12. L. W. Carlson and T. F. Irvine, Fully developed pressure drop in triangular ducts, *Trans. Am. Soc. Mech. Engrs* 60-WA-100 (1961).

MESURES D'ECOULEMENT TURBULENT DANS UN CONDUIT A SECTION TRIANGLE-RECTANGLE D'ANGLE 30/60

Résumé—On rapporte une étude expérimentale d'un écoulement turbulent établi dans un conduit rectiligne à section triangle-rectangle avec des angles internes de 60 et 30 degrés. Cette géométrie n'a pas de plans de symétrie et elle génère un type d'écoulement pour lequel on a peu de données. Les mesures sont faites avec un anémomètre à fil chaud. On présente le coefficient de frottement, les contours et les profils de vitesse axiale avec les contours et les profils d'intensité de turbulence, d'énergie cinétique de turbulence et de tension de Reynolds. Quand c'est possible, on compare les profils à ceux d'autres géométries de section. La présence et l'influence de la turbulence de l'écoulement secondaire sont dégagées et les circulations suivent les configurations obtenues dans des mesures antérieures avec d'autres conduits.

MESSUNGEN DER TURBULENTEN STRÖMUNG IN EINEM KANAL VON DREIECKIGEM QUERSCHNITT MIT DEN WINKELN 30/60/90 GRAD

Zusammenfassung—Es wird über Versuchsergebnisse in der vollständig entwickelten turbulenten Strömung in einem Kanal von dreieckigem Querschnitt mit den Winkeln 30, 60 und 90° berichtet. Diese Kanalgeometrie hat keine Symmetrieebenen, dadurch entsteht eine spezielle Art der Kanalströmung, für die nur spärlich Daten vorliegen. Die Messungen werden mit Hilfe eines Hitzdrahtanemometers in Luft ausgeführt, wozu eine besondere Versuchsanordnung gebaut worden ist. Als Ergebnis werden Widerstandsbeiwerte sowie axiale Geschwindigkeitsverteilungen vorgestellt, zusammen mit den Verteilungen der Turbulenzintensität, der turbulenten kinetischen Energie und den Reynolds'schen Schubspannungen. Wo immer dies möglich ist, werden die ermittelten Profile mit Meßergebnissen aus anderen Kanalgeometrien verglichen. Die Anwesenheit und der Einfluß von Sekundärströmungen infolge der Turbulenz sind klar erkennbar. Die Zirkulationsströmungen entsprechen den Formen, die aufgrund früherer Messungen in anderen Kanälen zu erwarten waren.

ИЗМЕРЕНИЕ ДЛЯ ТУРБУЛЕНТНОГО ТЕЧЕНИЯ В ПРЯМОМ КАНАЛЕ ТРЕУГОЛЬНОГО СЕЧЕНИЯ С ВНУТРЕННИМИ УГЛАМИ, СОСТАВЛЯЮЩИМИ 30 И 60 ГРАДУСОВ

Аннотация—Приводятся экспериментальные данные для полностью развитого турбулентного течения в прямом канале треугольного сечения, внутренние углы которого составляют 60 и 30 градусов. Такая геометрия канала не имеет плоскостей симметрии и приводит к образованию бесциркуляционного течения, для которого имеется недостаточное количество данных. Измерения проводятся при помощи термоанемометрии в устройстве для воздушного течения, специально сконструированном для опытов. Представлены характеристики коэффициента трения, а также контуры и профили осевой скорости наряду с контурами и/или профилями интенсивности турбулентности, кинетической энергии турбулентности и рейнольдсовских напряжений сдвига. В случаях, где это возможно, профили сравниваются с результатами измерений, проведенных в каналах других геометрий. Отчетливо выражено наличие и влияние вызванного турбулентностью вторичного течения в поперечной плоскости, и циркуляции течения соответствуют картине, ожилаемой в результате предыдущих измерений в других каналах.